



Cu/SiO₂ catalysts prepared by hom- and heterogeneous deposition–precipitation methods: Texture, structure, and catalytic performance in the hydrogenolysis of glycerol to 1,2-propanediol

Zhiwei Huang^{a,b}, Fang Cui^{a,b}, Jingjing Xue^a, Jianliang Zuo^a, Jing Chen^{a,b,*}, Chungu Xia^{a,b,*}

^a State Key Laboratory for Oxo Synthesis and Selective Oxidation, Lanzhou Institute of Chemical Physics, Chinese Academy of Sciences, Lanzhou 730000, China

^b Suzhou Institute of Nano-Tech and Nano-Bionics, Chinese Academy of Sciences, Suzhou 215123, China

ARTICLE INFO

Article history:

Received 27 April 2011

Received in revised form 22 August 2011

Accepted 22 August 2011

Available online 25 September 2011

Keywords:

Cu/SiO₂ catalyst

Deposition–precipitation method

Glycerol

Hydrogenolysis

Propanediol

ABSTRACT

Cu/SiO₂ catalysts prepared by homogeneous deposition–precipitation (Hom-DP) and heterogeneous deposition–precipitation (Het-DP) methods have been systematically characterized focusing on the effect of precipitation manner during catalyst preparation. It is found that the texture, structure and composition of the dried, calcined and reduced catalysts were largely affected by the precipitation manner. Based on characterizations and previous findings, the copper species on the dried, calcined, and reduced catalysts as well as on the catalysts after work were assigned. Due to a homogeneous precipitation manner, the catalyst prepared by Hom-DP method presented a much higher dispersion, a smaller copper particle size and thus a larger copper surface area than those of its counterpart prepared by Het-DP method. Unexpectedly, catalytic activity tests in the hydrogenolysis of glycerol showed that the catalyst prepared by Het-DP method inversely surpassed the former catalyst, mainly due to a larger number of copper species in the Het-DP catalyst was prerduced to active Cu⁰ sites, which also presented remarkably higher stability during aqueous phase glycerol reaction as compared to those in the former catalyst. In addition, the selectivity to 1,2-propanediol product is found to be affected by both the precipitation agent applied and the structure of the catalysts.

© 2011 Elsevier B.V. All rights reserved.

1. Introduction

Catalytic conversion of renewable biomass to fuels and commodity chemicals becomes more and more important because of the worldwide energy and environmental problems. Glycerol is one of the top-12 building block chemicals that can be derived from plant sources [1]. In addition, the production of biodiesel by the transesterification of vegetable oils and animal fats makes large quantities of glycerol available as a reaction co-product, ca. 10 wt% of the biodiesel produced. The availability and low cost of glycerol make it a promising feedstock for producing a wide range of value-added chemicals [2,3]. 1,2-Propanediol (1,2-PDO) is an important commodity chemical widely used for polyester resins, pharmaceuticals, foods, cosmetics and functional fluids, etc. Currently, 1,2-PDO is mainly produced by the hydration of propylene oxide from non-renewable petroleum derived propylene [2]. The production of 1,2-PDO from renewable glycerol by selective catalytic

hydrogenolysis of glycerol represents a low cost and green route for 1,2-PDO [4–22]. Noble metals such as Ru, Rh and Pt are extensively used in the hydrogenolysis of glycerol because of their high reactivity [7–10,13,16,19]. Nevertheless, these catalysts often promote excessive C–C cleavage, resulting in a poor selectivity to 1,2-PDO. Copper is known for its poor activity for C–C bond cleavage and high efficiency for C–O bond hydro-dehydrogenation [4,5,23]. Thus, as a less expensive alternative, copper is found to be potentially a good catalyst for the hydrogenolysis of glycerol. For example, over a copper-chromite catalyst Dasari et al. [5] converted glycerol to 1,2-PDO with 85% of 1,2-PDO selectivity at 55% of glycerol conversion under a mild condition of 1.4 MPa and 473 K. More recently, Cu–ZnO [20,21], Cu–Al₂O₃ [12,14] as well as Cu/ZnO/Al₂O₃ [11] catalysts are widely investigated at temperatures between 453 and 523 K due to their attractive performance in glycerol reaction.

In our previous work, we found that Cu/SiO₂ catalysts prepared by both impregnation and precipitation–gel (PG) methods showed high selectivity towards 1,2-PDO in the hydrogenolysis of glycerol with the catalyst prepared by the latter method exhibited much higher activity and better stability [24]. In addition, we have also found that the residual sodium in the Cu/SiO₂ catalysts prepared by PG method has profound effects on the structure and catalytic performance in the hydrogenolysis of glycerol of the

* Corresponding authors at: State Key Laboratory for Oxo Synthesis and Selective Oxidation, Lanzhou Institute of Chemical Physics, CAS, Lanzhou 730000, China. Tel.: +86 931 4968089; fax: +86 931 4968129.

E-mail addresses: chenj@lzb.ac.cn (J. Chen), cgxia@lzb.ac.cn (C. Xia).

catalyst [25]. Deposition–precipitation (DP) technique is a simple and convenient method widely used for the preparation of dispersed metal nanocatalysts [26–30]. It involves the suspension of a support material in the solution of a metal salt and the precipitation of the metal ions onto the support. Due to a different precipitation manner, this method can be divided into two parts: one is homogeneous deposition–precipitation (Hom-DP), in which metal ions were homogeneously precipitated by slowly hydrolysis of urea [26] or evaporation of ammonia [27,28]; and the other is heterogeneous deposition–precipitation (Het-DP), in which metal ions were quickly precipitated by an aqueous base solution [29,30]. Despite numerous researches on the preparation of dispersed nanocatalysts by DP method, few studies were focused on the differences in the structure and catalytic property of the catalysts prepared by different DP methods. Additionally, the catalytic performance of the Cu/SiO₂ catalysts prepared by DP method in the glycerol hydrogenolysis remains open to study. Accordingly, this work was undertaken with the aim of elucidating the differences in the structure and catalytic performance of the Cu/SiO₂ catalysts prepared by two different DP methods: one is the ammonia evaporation-based Hom-DP method, the other is the sodium hydroxyl precipitation-based Het-DP method. The structures of the catalysts were characterized by N₂ adsorption, N₂O chemisorption, infrared spectroscopy (FTIR), X-ray powder diffraction (XRD), simultaneous thermogravimetric/differential thermogravimetric analysis (TG–DTG), X-ray photoelectron spectroscopy (XPS), temperature-programmed reduction with H₂ (H₂-TPR), and transmission electron microscope (TEM). The relation between the catalytic performance for glycerol hydrogenolysis and the structure of the Cu/SiO₂ catalysts were discussed.

2. Experimental

2.1. Catalyst preparation

Hom-DP catalyst was prepared by homogeneous deposition–precipitation of the mixture of aqueous cuprammonia complex and silica sol. Briefly, a calculated amount of colloidal aqueous silica solution (SiO₂, 40.0 wt%, Guangzhou Renmin Chemical Plant, China) was added to the solution of cuprammonia complex (pH around 11). After stirring at room temperature for 3 h, the mixture was subsequently heated to 353 K and kept at this temperature for 20 h to evaporate ammonia. Then, the slurry of the gel was filtered, washed with hot distilled water, dried at 393 K overnight, and calcined at 723 K under air for 3 h.

Het-DP catalyst was prepared starting with a suspension of dried silica gel powder (Qingdao Haiyang Chemical Co., China, 442 m²/g, <100 mesh) in a solution of Cu(NO₃)₂ (0.5 mol/L). After stirring at room temperature for 3 h, Cu(NO₃)₂ solution was exclusively precipitated by adding an aqueous solution of NaOH (4 mol/L) till pH > 10. Then the temperature was raised to 353 K and kept at this temperature for 4 h. The resulted catalyst precursor was washed with distilled water until pH was 7 and then dried and calcined under the same conditions as that of Hom-DP catalyst. The metal loadings of the catalysts in terms of metal oxide were determined by X-ray fluorescence spectroscopy (XRF, PANalytical Magix PW 2403). Pure CuO reference was prepared by precipitating Cu(NO₃)₂ (0.5 mol/L) with the solution of NaOH (4 mol/L) and aged at 353 K for 4 h; after washing to pH = 7, the filter cake was dried and calcined as those of the silica containing samples.

2.2. Catalyst characterization

Fourier transform infrared (FTIR) spectra were recorded at room temperature on powdered samples using the KBr wafer technique

in a Nicolet Nexus 870 FTIR spectrometer. Simultaneous thermogravimetric/differential thermogravimetric (TG/DTG) experiments were performed on a Perkin-Elmer Pyris Diamond TG/DTA instrument in the temperature range 303–1273 K in N₂ atmosphere at a temperature ramp of 10 K/min.

The X-ray powder diffraction (XRD) of the samples was carried out on a PANalytical X'pert Pro Diffractometer using nickel filtered Cu K α radiation with a scanning angle (2θ) of 15–80° and a voltage and current of 40 kV and 30 mA. XRD patterns were also obtained during in situ reduction in 5% H₂/Ar at a flow rate of 50 mL/min up to 723 K. In these experiments the temperature was ramped between measurements at a rate of 10 K/min with a 5-min pause at each temperature before recording the pattern. The mean crystallite size of Cu was calculated by Scherrer equation according to the Cu(1 1 1) peak. X-ray photoelectron spectra (XPS) were obtained using a VG ESCALAB 210 spectrometer equipped with an Mg K α X-ray radiation source ($h\nu = 1253.6$ eV) and a hemispherical electron analyzer. All binding energies were calibrated using the Si2p peak at 103.4 eV as the reference.

Temperature-programmed reduction (TPR) measurements were carried out in a quartz U-tube reactor with 20 mg of sample used for each measurement. The samples were first pretreated at 473 K under He flow for 1 h and then samples were reduced with 20% H₂/Ar at a flow rate of 50 mL/min and the temperature was increased from 303 K to 773 K at a ramping rate of 10 K/min. H₂ consumption was continuously monitored by a thermal conductivity detector (TCD).

The dispersion of the catalysts was determined by dissociative N₂O chemisorption [31]. The catalysts were first reduced at 773 K with 20% H₂/Ar at a flow rate of 50 mL/min for 1 h. After cooling to 363 K in a He flow, the reduced samples were exposed to a 5% N₂O/N₂ mixture (50 mL/min) for 0.5 h. Finally, the samples were cooled to room temperature to start another TPR run with 20% H₂/Ar at a flow rate of 50 mL/min and a ramping rate of 10 K/min to 573 K. The copper metallic surface area, average copper particle size and dispersion were calculated by assuming 1.4×10^{19} copper atoms per m² and a molar stoichiometry N₂O/Cu_s = 0.5, where the symbol Cu_s means the copper atoms on the surface [31,32].

The BET surface area measurements were performed on a Micromeritics ASAP 2010 instrument at liquid nitrogen temperature. Prior to measurements, the samples were degassed at 473 K overnight. Transmission electron microscopic (TEM) investigations were carried out using a JEM2010 electron microscope at 200 kV.

2.3. Catalytic activity testing

The glycerol reaction was carried out in a 200 mL stainless steel autoclave at a stirring speed of 400 rpm. Prior to the reaction, the catalysts were prerduced by H₂ stream at 553 K for 3 h. The standard reaction was carried out under the following reaction conditions: 6.4 MPa of initial H₂ pressure, 80 g of 80 wt% glycerol aqueous solution, 4 g of reduced catalyst, 12 h. After being purged, the reactor was heated to the reaction temperature, and the H₂ pressure was increased to about 9.0 MPa and maintained during the reaction. The liquid phase products were analyzed by using a gas chromatograph with a SE-54 capillary column (50 m \times 0.32 mm) and a flame ionization detector. The gas products were analyzed by using a gas chromatograph (Porapak Q column (4 m \times 3 mm)) equipped with a TCD. Products were also identified on a HP 6890/5793 GC-MS with a DB-5MS column. The detected liquid products were methanol, ethanol, 2-propanol, 1-propanol, acetol, ethylene glycol (EG), 1,2-PDO and 1,3-PDO, and a typical gas chromatogram of these products is shown in Fig. 1. The detected gas products were small amount of CH₄ and CO₂. Conversion of the

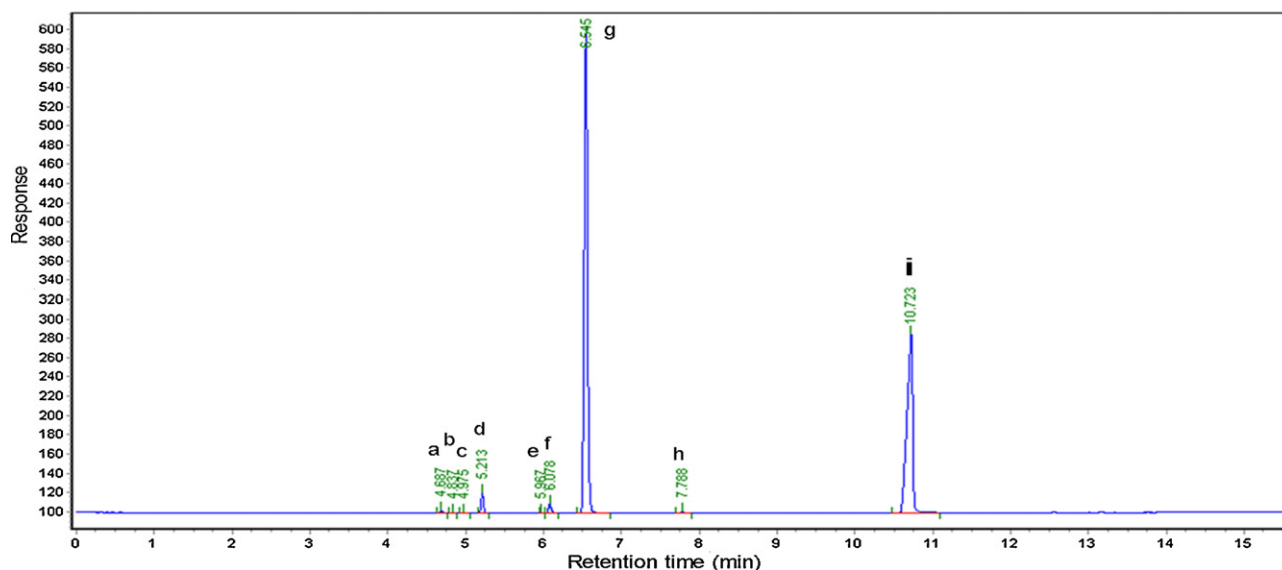


Fig. 1. Gas chromatogram of the hydrogenolysis reaction products: (a) methanol; (b) ethanol; (c) 2-propanol; (d) 1-propanol; (e) acetol; (f) EG; (g) 1,2-PDO; (h) 1,3-PDO; (i) glycerol.

glycerol was calculated on the basis of the following equation:

$$\text{conversion(\%)} = \frac{\text{sum of C-based moles of all products}}{\text{sum of C-based moles of reactant and all products}} \times 100$$

The selectivity of the products was calculated based on a carbon basis:

$$\text{selectivity(\%)} = \frac{\text{C-based moles of specific products}}{\text{sum of C-based moles of all products}} \times 100$$

3. Results and discussion

3.1. Structure properties

FTIR experiments were carried out to study the structure and composition of the dried and calcined samples prepared by different DP methods. For dried Hom-DP sample (Fig. 2(A)), the apparent absorption bands at approximately 1120, 800, and 476 cm^{-1} are assigned to the different vibration modes of the Si–O bonds in the amorphous SiO_2 [33,34]. The shoulder peak at around 1046 cm^{-1} on the low-frequency side of the ν_{SiO} band at 1120 cm^{-1} together with the presence of the weak δ_{OH} band at around 670 cm^{-1} indicates the presence of copper phyllosilicate [33]. In addition, a small absorption at 1384 cm^{-1} related to NO_3 groups is also observed in the profile of the dried Hom-DP sample, suggesting that a small amount of $\text{Cu}_2(\text{OH})_3\text{NO}_3$ is also present [33]. For dried Het-DP sample the broad bands at around 1028 and 670 cm^{-1} can be ascribed to the ν_{SiO} and the δ_{OH} band of copper phyllosilicate (Fig. 2(C)), respectively. It should be noted here that an attenuated shoulder peak at around 690 cm^{-1} characteristic of the δ_{OH} vibration of $\text{Cu}(\text{OH})_2$ is also observed [33]. More evidence for the presence of $\text{Cu}(\text{OH})_2$ in the dried Het-DP sample will be given below. $\text{Cu}(\text{OH})_2$ is reported to form in the dried catalyst precursor prepared by ammonia evaporation-based Hom-DP method analogy to this work [28]. Therefore, the formation of a small amount of $\text{Cu}(\text{OH})_2$ in the dried Hom-DP sample can not be excluded.

After calcination at 723 K, the absorption band associated with NO_3 groups in Hom-DP sample disappeared, and at the same time both the δ_{OH} band at ~ 670 cm^{-1} and the ν_{SiO} shoulder at 1046 cm^{-1} associated with copper phyllosilicate slightly decreased (Fig. 2(B)).

These findings suggests that $\text{Cu}_2(\text{OH})_3\text{NO}_3$ species in this sample completely decomposed to CuO after calcination while the structure of copper phyllosilicate was mainly preserved. In contrast, for calcined Het-DP sample, the ν_{SiO} band at 1027 cm^{-1} shifted to 1097 cm^{-1} and the broad δ_{OH} band at ~ 670 cm^{-1} almost disappeared, indicating that copper phyllosilicate in this sample largely decomposed into silica and CuO . In addition, the shoulder peak at 690 cm^{-1} presented in the dried Het-DP sample completely disappeared, suggesting the full decomposition of $\text{Cu}(\text{OH})_2$. The formation of CuO after calcination in this sample is also confirmed by XRD pattern given below.

Fig. 3 illustrates the TG–DTG curves of the dried precursors of Hom-DP and Het-DP catalysts, which revealed that the decomposition of both samples occurred in three main weight loss steps. The first weight loss step at temperatures below 400 K for both samples can be attributed to the removal of weakly bonded water,

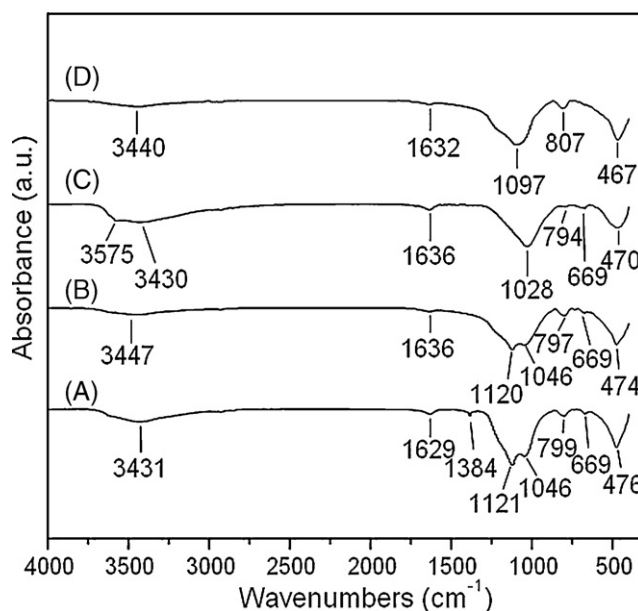


Fig. 2. FTIR spectra of: (A) dried Hom-DP sample; (B) calcined Hom-DP sample; (C) dried Het-DP sample and (D) calcined Het-DP sample.

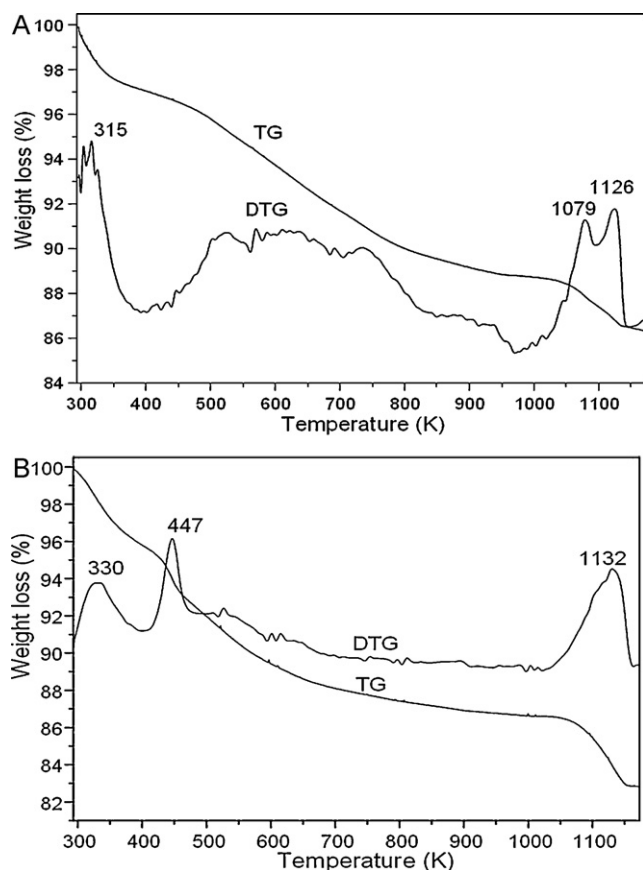


Fig. 3. TG–DTG curves of the dried precursors of Hom-DP (A) and Het-DP (B).

while the second weight loss step in the range 400–950 K is likely associated with the decomposition of different copper species (copper phyllosilicate and $\text{Cu}(\text{OH})_2$ in the dried Het-DP sample; copper phyllosilicate, $\text{Cu}(\text{OH})_2$ and $\text{Cu}_2(\text{OH})_3\text{NO}_3$ in the dried Het-DP sample) and the dehydration of silanol groups in the samples. The obvious weight loss peak observed in the DTG curve of Het-DP sample at around 447 K is associated with the decomposition of copper hydroxide in the dried precursor of this sample, as the decomposition of which usually occurs in the range of 413–473 K [35]. The decomposition extent of copper phyllosilicate is reported to depend on the preparation conditions and the thermal pretreatment. Toupance et al. [36] revealed a partial decomposition of copper phyllosilicate when being calcined at 723 K, while Yurieva et al. [37] reported that the copper phyllosilicate prepared by urea hydrolysis-based Hom-DP method is stable up to a calcination temperature of 900 K and then decomposed to CuO and silica after calcination at 1023 K. In addition, the decomposition of CuO to Cu_2O is reported to occur at a high temperature of around 1100 K [35]. Thus, it is reasonable that the third profound weight loss of Hom-DP sample, which is composed of two overlapped processes as indicated from the DTG curves, is associated with the full decomposition of copper phyllosilicate to CuO and silica (at 1079 K) and the degradation of CuO to Cu_2O (at 1126 K). Similarly, the broad weight loss peak of Het-DP sample in the range of 1000–1173 K is possibly attributed to the collective contribution of the decomposition of copper phyllosilicate and CuO .

XRD diffraction patterns were taken for both the dried and calcined samples prepared by different DP methods. For dried Het-DP sample (Fig. 4(A)), weak and diffused diffractions characteristic of CuO have already appeared at $2\theta = 35.5^\circ$ and 38.7° (JCPDS 05-0661). It seems that a part of $\text{Cu}(\text{OH})_2$, which is formed by precipitation of $\text{Cu}(\text{NO}_3)_2$ with NaOH , is unstable and decomposed to CuO during

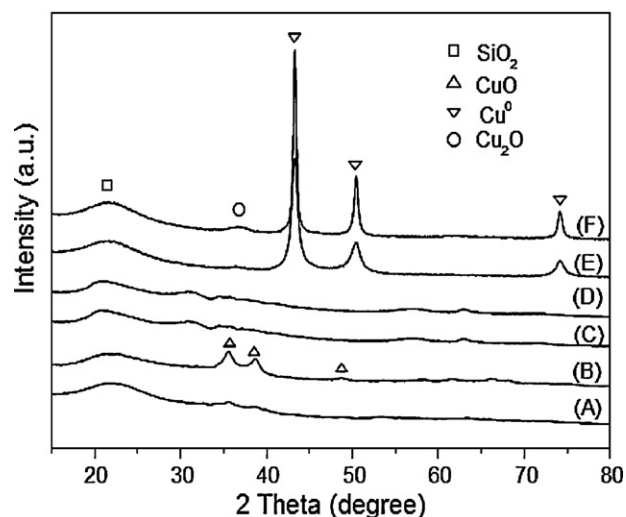


Fig. 4. XRD patterns of: (A) dried Het-DP sample; (B) calcined Het-DP sample; (C) dried Hom-DP sample; (D) calcined Hom-DP sample; (E) used Het-DP sample and (F) used Hom-DP sample.

the aging and drying processes. The diffraction peaks of CuO further intensified after calcination (Fig. 4(B)). The apparent feature of dried Hom-DP sample was the broad and diffused diffraction of amorphous silica at around $2\theta = 22^\circ$ (Fig. 4(C)). In addition, the weak and diffuse diffraction peaks at ca. 31.2° and 35.8° suggest the presence of copper phyllosilicate with poor crystallinity [28,33]. No big difference was seen after calcined at 723 K, suggesting the high stability of copper species in Hom-DP sample (Fig. 4(D)). After glycerol reaction at 473 K, sharp and intensified diffraction peaks of metallic copper were seen in the used Hom-DP catalyst (Fig. 4(F)). In contrast, the diffraction peaks of Cu^0 in the used Het-DP catalyst are much lower and broader (Fig. 4(E)). These findings suggest that copper species in Hom-DP catalyst were seriously aggregated to much larger particles (21.0 nm) during glycerol reaction as compared to Het-DP catalyst, which is 10.8 nm (almost one half that of used Hom-DP catalyst). In addition, a broad diffraction peak at around $2\theta = 36.8^\circ$ attributed to Cu_2O is also observed in both samples, and its diffraction is more intense for Hom-DP catalyst than for Het-DP catalyst, indicating the presence of a larger amount of Cu_2O phase in the former catalyst.

In situ XRD diffraction patterns were taken during the reduction of the calcined samples. At temperature below 473 K, no obvious change was observed in the XRD pattern of Hom-DP sample (Fig. 5(A)). With increasing temperature up to 473 K, broad and clear diffraction peaks characteristic of metallic Cu appeared. The diffraction peaks of copper slightly intensified with no distinct increase in the amplitude of the diffraction peaks even up to 723 K. The in situ reduction profiles of calcined Het-DP sample showed that this sample is stable at temperature below 448 K (Fig. 5(B)). After reduction at 473 K, a weak but observable peak appeared in between the diffraction peaks of CuO at $2\theta = 35.5^\circ$ and 38.6° , it may associate with the presence of Cu_2O , more evidence for the presence of this species will be given below. When the temperature raised up to 498 K, the diffraction peaks associated with Cu^0 appeared with no additional CuO and Cu_2O phases detectable, indicating that copper species were mainly reduced to Cu^0 at this temperature. Note that the full presence of the diffractions of Cu^0 for Hom-DP sample occurred at a temperature around 25 K lower than Het-DP sample, suggesting that the reduction of the majority of copper species in the calcined Het-DP occurred at temperature a bit higher than Hom-DP sample. Only slightly intensified diffraction peaks of Cu^0 were seen with further increasing reduction temperature to 723 K. It should be noted here that although there

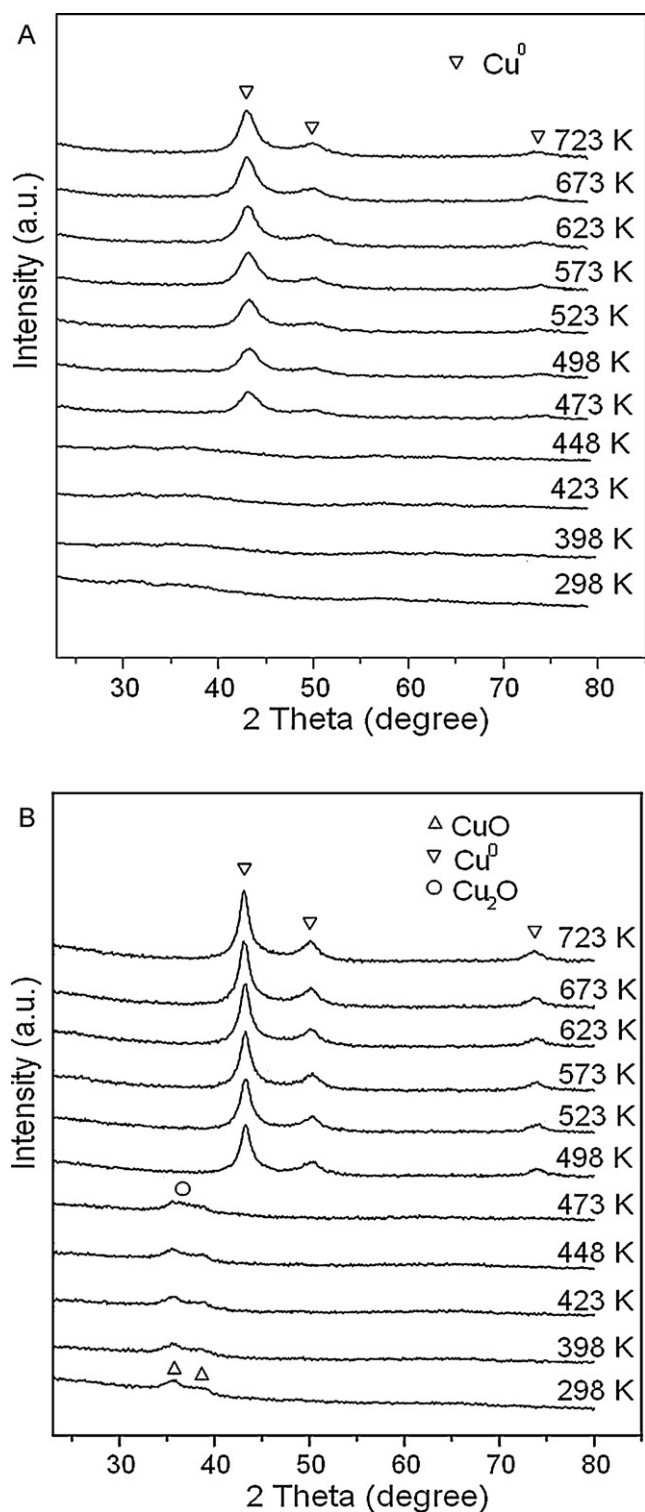


Fig. 5. In situ XRD patterns taken during reduction of calcined Hom-DP (A) and calcined Het-DP (B).

was no detection of the diffraction of Cu_2O in the XRD patterns of both samples after reduction to temperatures above 498 K, it does not mean that copper species in both samples have been fully reduced to Cu^0 at this temperature, because Cu_2O species with high dispersion and/or small amount are likely to be X-ray amorphous.

Both Hom-DP and Het-DP catalysts showed remarkably high stability during the reduction process as the crystallite sizes of copper for Hom-DP and Het-DP just increased from 4.2 to 4.7 nm and

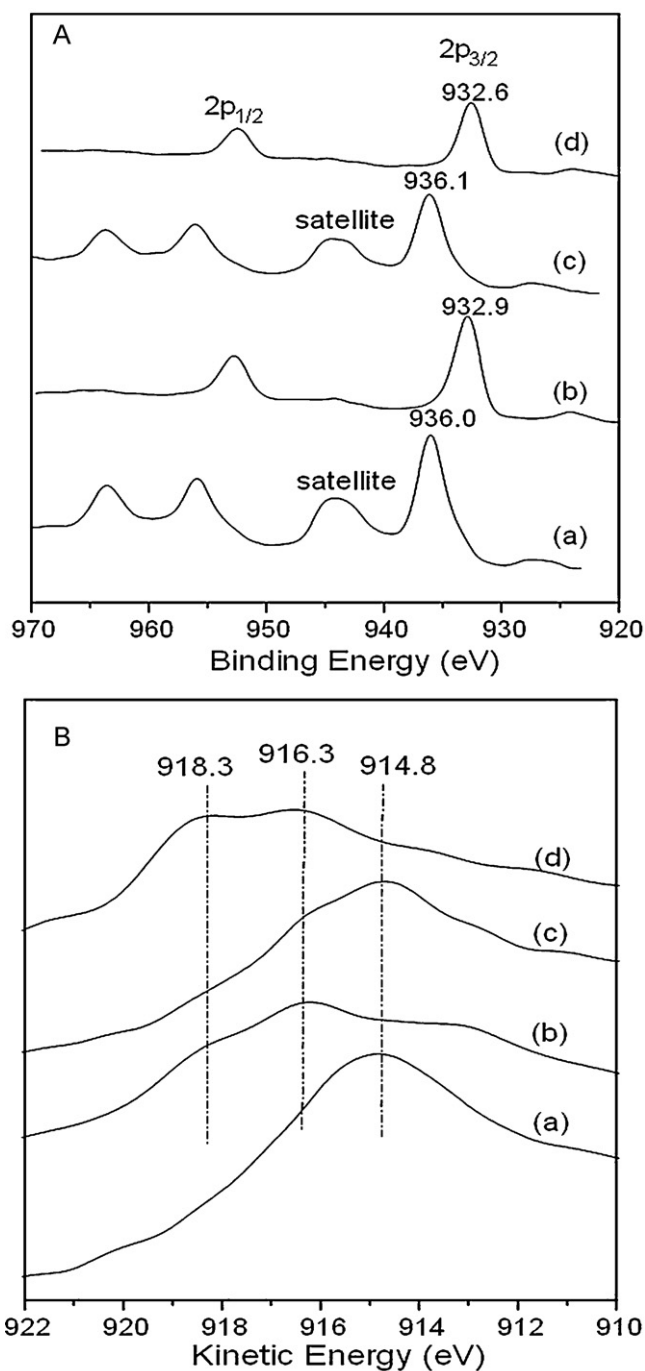


Fig. 6. XPS spectra of calcined and used Hom-DP and Het-DP catalysts: (A) Cu2p spectra and (B) Cu LLM Auger kinetic energy of (a) calcined Hom-DP; (b) used Hom-DP; (c) calcined Het-DP and (d) used Het-DP.

from 6.1 to 7.0 nm, respectively, with increasing reduction temperature from 498 to 723 K.

XPS experiments were carried out to determine the oxidation state of copper as well as the chemical compositions of the samples. The high values of the binding energy (BE) (>936.0 eV) along with the presence of the characteristic shakeup satellite peaks suggest that the copper oxidation state is +2 in both samples (Fig. 6(A)) [38]. The BE of pure CuO prepared by precipitation was determined at 934.0 eV. Thus, the relatively large positive BE shift of the Cu2p core level for the DP samples is indicative of a charge transfer from the metal ions towards the support matrix [39]. Van Der Grift et al. [26] found that no copper (II) oxide but copper phyl-

Table 1
XPS analysis of CuO/SiO₂ catalysts prepared by different methods.

Catalyst		Position of Cu2p _{3/2} (eV)	Cu/Si atoms ratio	
			Bulk	XPS
Hom-DP	Fresh	936.0	0.331	1.275
	After work	932.9	–	0.374
Het-DP	Fresh	936.1	0.339	0.913
	After work	932.6	–	0.329

losilicate was present in the calcined CuO/SiO₂ samples prepared by urea hydrolysis-based Hom-DP method by XPS, as the BE of the latter species is 2.0 eV higher than that of the former. Chen et al. [28] also ascribed the higher BE of the CuO/SiO₂ samples prepared by ammonia evaporation-based Hom-DP method analogy to this work at higher evaporation temperature to the presence of copper phyllosilicate. Therefore, the high BE of both Hom-DP and Het-DP samples can also be ascribed to the formation of copper phyllosilicate, the presence of which was confirmed by FTIR analysis (Fig. 2). The XPS surface Cu/Si atom ratios on Het-DP and Hom-DP samples are 2.7 and 3.8 times higher than their corresponding bulk ratios, respectively, suggesting copper species on both samples are largely enriched on the surface [40].

After work, the BE of Cu2p_{3/2} core levels of both catalysts reduced to 932.6–932.9 eV and the characteristic shakeup satellite lines of Cu²⁺ disappeared, indicating that copper became reduced (Cu⁺ or Cu⁰). Because the BE values of Cu⁺ and Cu⁰ are almost identical, the distinction between these two species present on the catalyst surface is feasible only through the examination of the Auger spectra [34,41]. Two overlapping Cu LMM Auger kinetic energy peaks centered at about 918.3 and 916.3 eV are observed in the used Hom-DP and Het-DP catalysts (Fig. 6(B)), characterizing the coexistence of both Cu⁰ and Cu⁺ on the surface. As can be seen from the Auger kinetic energy profiles of the used catalysts, the peak at 916.3 eV is more apparent for Hom-DP catalyst, while the peak at 918.3 eV is more prominent for Het-DP catalyst. These findings suggest that Cu⁺ species was the major species in the used Hom-DP catalyst while Cu⁰ was the major species present in the used Het-DP catalyst [29,41]. It is reported that when copper is highly dispersed and in intimate contact with the supports, Cu2p_{3/2} energies, particularly Cu Auger parameters, may deviate significantly from the corresponding bulk values [29]. The large negative shift of Cu LMM Auger kinetic energy for both calcined DP catalysts implied the difference in copper coordination. After reaction, a more profound decrease of Cu/Si ratio for the used Hom-DP catalyst (from 1.275 to 0.374) as compared to Het-DP catalyst (from 0.913 to 0.329) was seen (Table 1), suggesting a more serious aggregation of copper in the former catalyst during glycerol reaction. The above findings are in good agreement with the XRD results shown in Fig. 4(E and F).

From the above characterizations, we know that due to a different precipitation manner, different copper species are present in both the dried and calcined samples. In addition, grafted Cu²⁺ ions, which are formed by electrostatic adsorption of Cu^{II} cations with the negatively charged silica particles [33] and cannot be tracked by the above characterizations, may also selectively form in the DP samples. In Cu/SiO₂ catalyst prepared by Het-DP, the pH of the solution is increased from around 3 to above 10 with the dropping of NaOH. At a low initial pH, the silica surface is positively charged. Thus, it is not favorable for Cu^{II} cations to adsorb on silica surface to form grafted Cu²⁺ ions. With increasing pH, Cu^{II} cations were precipitated to Cu(OH)₂ nanoparticles. Cu(OH)₂ nanoparticles would further react with the silica surface to form copper phyllosilicate in a high pH solution [33]. Therefore, both Cu(OH)₂ and copper phyllosilicate coexist in the dried Het-DP, besides CuO (which is formed by the decomposition of Cu(OH)₂ during high temperature aging and drying). Differently, in the catalyst prepared

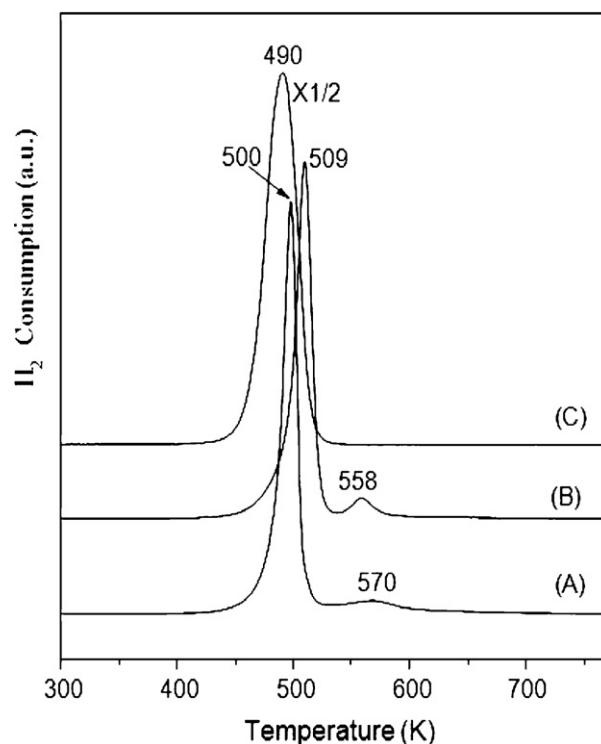


Fig. 7. H₂-TPR profiles of calcined Hom-DP sample (A); calcined Het-DP sample (B) and the reference sample pure bulk CuO (C).

by Hom-DP, the initial pH is around 11, the silica surface is negatively charged, favoring the adsorption of copper cations. With the decrement of the pH of the suspension by evaporation of ammonia, Cu(OH)₂ may form and it would further react with the silica surface to form copper phyllosilicate. With further decreasing of pH, copper nitrate hydroxide may also form, as which is reported to precipitate at 7 < pH < 8.8 [33]. Thus we suggest that on dried Cu/SiO₂ samples prepared by Hom-DP method, besides the presence of copper nitrate hydroxide (identified by FTIR) and copper phyllosilicate (identified by FTIR and XRD), there are a small amount of highly dispersed Cu(OH)₂ and grafted Cu²⁺ ions. After calcination, both CuO, which comes from the decomposition of Cu(OH)₂ and copper phyllosilicate, and undecomposed copper phyllosilicate coexist in Het-DP sample. For calcined Hom-DP sample, there are three kinds of copper species: copper phyllosilicate, isolated-grafted Cu²⁺ ions and a small amount of highly dispersed CuO (originating from the full decomposition of Cu(OH)₂ and Cu₂(OH)₃NO₃, and the partial decomposition of copper phyllosilicate).

Fig. 7 shows the TPR profiles of the calcined Hom-DP and Het-DP samples along with the reference unsupported bulk CuO. As can be seen, Hom-DP catalyst is reduced in a much wide range from 410 to 642 K with a main reduction peak centered at 500 K and a broad shoulder peak centered around 570 K. Similar to Hom-DP catalyst, Het-DP sample also showed two reduction peaks with the main peak present at 509 K and the shoulder peak at 558 K. Differently, unsupported pure CuO showed a good symmetric hydrogen consumption peak centered around 490 K, which is 10–20 K lower than that of the main peak of DP samples, showing clearly the inhibit effect of the silica particles in the reduction of Cu²⁺ species.

As it is well known, dispersed CuO with small particle sizes can be more facily reduced to Cu⁰ than did the bulk CuO with larger sizes [38,42]. In contrast, dispersed and surface interacted Cu²⁺ species are reported to be more difficult to reduce than bulk CuO [43,44]. Thus, the above mentioned inhibiting effect of the silica particles in the reduction of the DP samples would probably be due

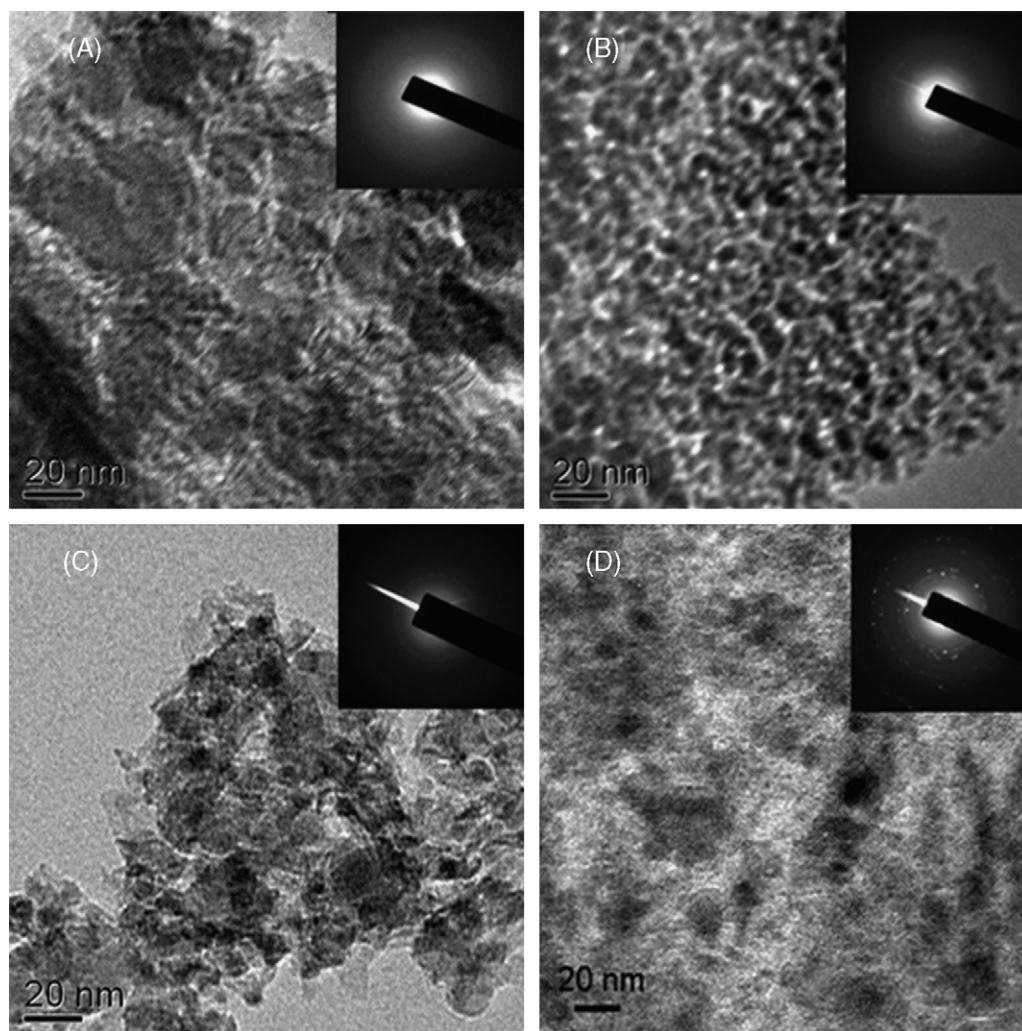


Fig. 8. TEM images of calcined and reduced samples (A) calcined Hom-DP sample; (B) calcined Het-DP sample; (C) reduced Hom-DP sample; and (D) reduced Het-DP sample.

to the presence of the surface interacted Cu^{2+} species, that is copper phyllosilicate in calcined Het-DP sample, copper phyllosilicate and grafted Cu^{2+} ions in calcined Hom-DP sample [28]. Therefore, it is reasonable that the main reduction peak of the CuO/SiO_2 samples is attributed to the collective contribution of stepwise reduction of dispersed CuO to Cu^0 (from in situ XRD results) and the partially reduction of surface interacted Cu^{2+} species to Cu^+ ; while the shoulder peak in the high temperature range is ascribed to the reduction of supported Cu^+ , which is derived from the stepwise reduction of surface interacted Cu^{2+} species. Thus, a small proportion of Cu_2O with high dispersion tracked by H_2 -TPR is inferred to present in the in situ XRD reduction experiments of both samples, and it would still exist after the full presence of Cu^0 diffraction peaks.

The textural properties of both calcined catalysts including the specific surface area, average pore diameter, metal dispersion, metal surface area, and copper particle size are summarized in Table 2. Both catalysts showed high specific BET surface areas of

above $330 \text{ m}^2/\text{g}$ with the calcined Hom-DP much higher, which is $366 \text{ m}^2/\text{g}$. The pore volume of both catalysts is in the range of $0.72\text{--}0.85 \text{ cm}^3/\text{g}$. The copper dispersion of the catalysts obtained from N_2O chemisorption for Hom-DP catalyst is also higher than that of Het-DP catalyst, which is in consistent with the results obtained from XRD and XPS. As a result of copper dispersion, Hom-DP catalyst presented a much higher copper surface area and a lower copper particle size than those of the Het-DP catalyst.

Fig. 8 shows the TEM images of the calcined and reduced samples prepared by different DP method. In calcined Hom-DP sample (Fig. 8(A)), randomly oriented filandrous species, which can be assigned to copper phyllosilicate according to literature [28] and the above characterizations, along with a few dark particles with much small sizes assignable to CuO are observed. The highly diffuse ring pattern in the select area electron diffraction (SAED) of this sample reveals an amorphous structure. For calcined Het-DP sample, dark gray particles with quasi-spherical shape can be assigned

Table 2

The texture of the calcined samples prepared by Hom-DP and Het-DP methods.

Catalyst	CuO^a (wt%)	BET surface area ^b (m^2/g)	VP^b (cm^3/g)	Cu-dispersion ^c (%)	Cu-metal area ^c (m^2/g)	Copper particle size ^c (nm)
Hom-DP	30.5	366	0.72	24.6	165.1	4.1
Het-DP	31.0	334	0.85	16.2	109.6	6.2

^a Measured by XRF.

^b BET method.

^c Calculated from dissociative N_2O adsorption.

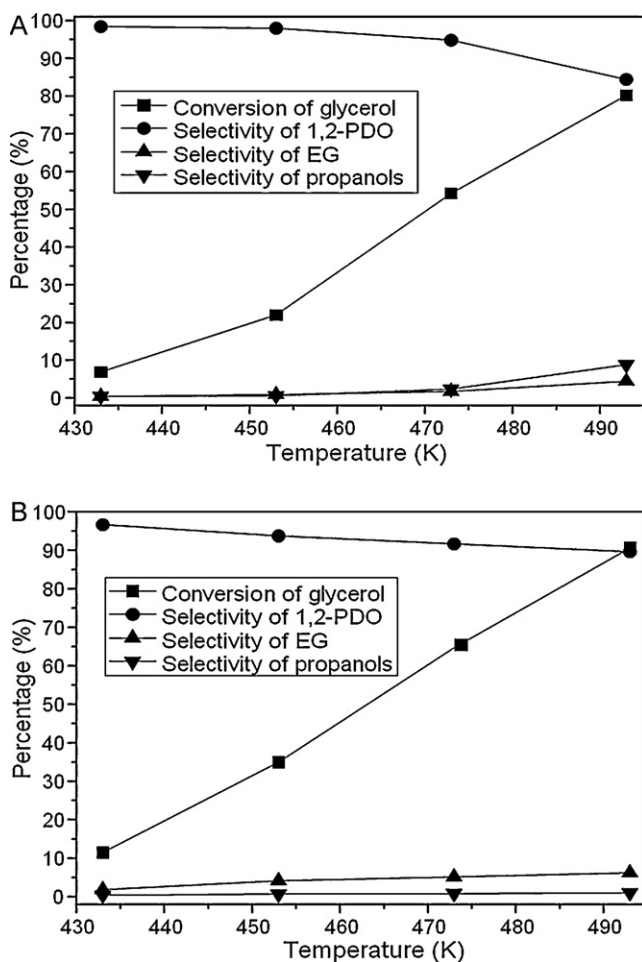


Fig. 9. Catalytic activity and selectivity of the reduced Hom-DP (A) and Het-DP (B) catalysts as a function of temperature. Reaction conditions: 80% aqueous solution of glycerol 80 g, total pressure 9.0 MPa, reduced catalyst 4 g, 12 h (propanols = 1-propanol + 2-propanol).

to CuO, which exhibit a narrow size distribution of 2–9 nm with an average diameter of around 6 nm. The inset in Fig. 8(B) shows a corresponding SAED pattern of this sample, in which a few scattered spots are occasionally observed, characterizing of highly dispersed or amorphous samples with poor crystalline.

After reduction at 553 K, the filamentous morphology of the copper phyllosilicate in Hom-DP was to some extent retained (Fig. 8(C)). In addition, a few dark particles with an average diameter of 6 nm due to the presence of Cu⁰ are also observed in this sample. Differently, many black quasi-spherical particles attributable to metallic Cu emerged in the reduced Het-DP sample (Fig. 8(D)). The particles showed a wider size distribution of 3–16 nm with an average size of about 9 nm. The metallic Cu particle sizes observed by TEM are larger than the crystallite sizes derived from in situ XRD, indicating the polycrystalline nature of the metallic Cu particles.

3.2. Catalytic performance

The catalytic activity and selectivity of both catalysts as a function of temperature are given in Fig. 9. As can be seen, the conversion of glycerol for both catalysts steadily increased with increasing temperature, with the activity of Het-DP catalyst 4–12% higher than that of Hom-DP catalyst at each temperature point investigated. The selectivity to 1,2-PDO is a little bit complex. At temperatures below 473 K, the selectivity to

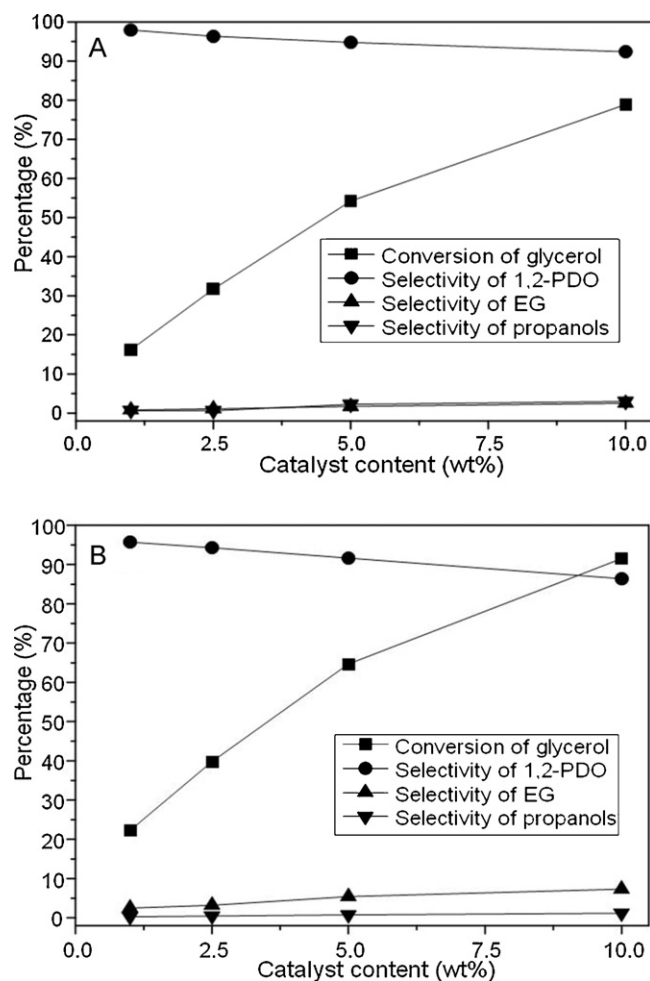


Fig. 10. Effect of catalyst amount on the glycerol reaction over reduced Hom-DP (A) and Het-DP (B) catalysts. Reaction conditions: 80% aqueous solution of glycerol 80 g, total pressure 9.0 MPa, 473 K, 12 h (propanols = 1-propanol + 2-propanol).

1,2-PDO for Hom-DP catalyst was 1.8–4.3% higher than that of Het-DP catalyst; at temperature above 473 K, the selectivity to 1,2-PDO for Hom-DP sharply decreased to a value of 5% lower than that of Het-DP catalyst. With increasing temperature, both the selectivity to EG and propanols smoothly increased, and a sharp increase of propanols byproducts from 2.3% at 473 K to 8.8% at 493 K was seen over Hom-DP catalyst. The formation of a large number of extensive hydrogenolysis products of propanols explained the sharp decrease of 1,2-PDO selectivity of Hom-DP catalyst at 493 K [7]. The space-time-yield (STY) of 1,2-PDO for Het-DP and Hom-DP catalysts are calculated to be 2.6 and 2.2 g_{1,2-PDO} g_{Cu}⁻¹ h⁻¹ at 473 K, respectively. Although the STY values of Het-DP and Hom-DP catalysts are lower than that of the copper based state-of-the-art catalysts for the same reaction reported by Bienholz et al. over a CuO/ZnO prepared by an oxalate gel method [20], which is 9.8 g_{1,2-PDO} g_{Cu}⁻¹ h⁻¹ at the same reaction temperature, they are higher than those of the CuO/ZnO prepared by coprecipitation [45] and Cu/Al₂O₃ catalyst prepared by impregnation method [14], which produce 1,2-PDO with STYs of 0.8 and 1.9 g_{1,2-PDO} g_{Cu}⁻¹ h⁻¹, respectively.

Fig. 10 shows the effect of catalyst amount on glycerol reaction over the prerduced Hom-DP and Het-DP catalysts at 473 K. As can be seen, the conversions of glycerol increased 4 to 5 fold with the increase of catalyst amount from 1 wt% to 10 wt% for both catalysts, and the higher the amount of the catalyst, the larger the activity of Het-DP catalyst is over Hom-DP catalyst. The selectivity to 1,2-PDO for Hom-DP catalyst slightly decreased from 97.8% to 92.4%, while a large decrease of 1,2-PDO selectivity from 96.0% to 86.4% was seen

Table 3
Studies of the reuse of Hom-DP and Het-DP catalysts.

Catalyst	Hom-DP		Het-DP	
	Conversion (%)	Selectivity (%)	Conversion (%)	Selectivity (%)
First time	22.1	98.0	35.0	93.7
Second time	11.7	97.8	30.1	95.2
Third time	6.1	98.4	21.6	96.0

Reaction conditions: 80% aqueous solution of glycerol 80 g, 453 K, total pressure 9.0 MPa, reduced catalyst 4 g, 12 h.

over Het-DP catalyst with increasing catalyst concentration. The increase in conversion with the increase in catalyst concentration could be due to the more availability of active sites for the reaction which also leads to the excessive degradation of glycerol reactant and hydrogenation of 1,2-PDO product to lower alcohols.

To study the recycle ability as well as the deactivation behavior of the catalysts, both catalysts were also used to carry out the recycle experiments at 453 K (Table 3). After reaction, the freshly used catalysts were filtrated and recharged into the autoclave together with the fresh reactant to perform the next run. After recycle serious loss of activity was observed over Hom-DP catalyst, as nearly one half of the initial activity was lost (decreased from 22.1% to 11.7%). Het-DP catalyst presented moderately good stability, its activity just declined from 35.0% to 30.1% after the second run. The activity of both catalysts further decreased after the third run, however, the activity of Het-DP catalyst is still maintained almost equal to that of the fresh Hom-DP catalyst, showing a higher stability of the former catalyst. The selectivity to 1,2-PDO for Hom-DP catalyst maintained at around 98.0% without big change after three-run catalytic cycles, whereas a slight increase of selectivity was seen for Het-DP catalyst after recycle (Table 3).

From the above characterizations, we know that the catalyst prepared by Hom-DP method exhibited a higher dispersion, a lower copper domain and thus a larger copper surface area than those of the catalyst prepared by Het-DP method. Nonetheless, the situation is opposite after reaction. XRD characterization of the used samples (Fig. 4(E and F)) showed that the particles of Cu⁰ in Hom-DP catalyst significantly sintered to much large aggregates, while those particles in Het-DP were reasonably stable. XPS results also revealed a more serious aggregation of copper in the Hom-DP catalyst after reaction (Table 1). The poor stability of copper in the prereduced Hom-DP catalyst during the aqueous phase glycerol hydrogenolysis reaction would be the major reason for the inferior performance (lower activity, poorer recycle stability) of this catalyst. After reaction, the leaching of Cu²⁺ as measured by atomic absorption spectrometry (AAS) is 13.0 μg/g for Hom-DP catalyst and 2.8 μg/g for Het-DP catalyst. In our previous report [25] we found that the leaching of Cu²⁺ during glycerol reaction could inhibit the activity of the Cu/SiO₂ catalyst prepared by PG method. Thus, the much serious leaching of Cu²⁺ would also reduce the activity of the Hom-DP catalyst, and be another reason for the lower activity of this catalyst.

From the above H₂-TPR characterizations (Fig. 7), we know that it requires a high temperature of above 615 K for calcined Het-DP sample and 642 K for calcined Hom-DP sample to be fully reduced to Cu⁰. Thus, under a low prereduction temperature of 553 K, a proportion of hard-reducible copper species in both samples would just be inadequately reduced to Cu⁺ species rather than Cu⁰. In our previous work [24], we found that Cu⁺ species is not likely formed during glycerol reaction but rather formed during the prereduction treatment. In this work, the Cu₂O species detected in the used samples by both XRD and XPS is probably formed by the aggregation of the highly dispersed Cu₂O in the inadequately reduced catalysts during the high temperature glycerol reaction. Based on the above XRD (Fig. 4(E and F)) and XPS (Fig. 6) characterizations, a larger amount of Cu₂O species are found in the used Hom-DP catalyst. Thus, a large

amount of Cu₂O species are inferred to exist in the 553 K prereduced Hom-DP sample than in Het-DP sample. Previously, we reported that the Cu⁰ formed during the prereduction treatment and/or generated in situ during the reaction is the active site for glycerol reaction, while the Cu⁺ species formed during the prereduction treatment might be catalytically inactive in glycerol reaction [24]. Thus, in the present work, the presence of a larger amount of Cu₂O species in Hom-DP sample would also to some extent result in the lower activity of this sample as compared to Het-DP sample.

In our previous work [25] we found that the incorporating of Na is one of the main reasons for the degradation of glycerol to EG byproduct over copper catalysts prepared by precipitation with sodium-containing bases. In the present work, a higher selectivity to 1,2-PDO product and a lower selectivity to EG byproduct are found over Hom-DP catalyst than over Het-DP catalyst at temperature below 473 K, probably due to the free of sodium residual in the former catalyst. In addition, a sharp decrease of 1,2-PDO selectivity of Hom-DP catalyst from 473 K to 493 K due to the formation of a large number of extensive hydrogenolysis products of propanols was seen. As known from the above XRD and XPS characterizations, the structure of Hom-DP catalyst significantly changed during the aqueous phase glycerol reaction, and small copper particles in the reduced Hom-DP catalyst profoundly sintered to large aggregates. In contrast, the structure of Het-DP catalyst was reasonably stable. Thus, the sharp decrease of 1,2-PDO selectivity due to extensive hydrogenolysis would be aroused by the profound structure change of Hom-DP catalyst during the aqueous phase glycerol reaction.

4. Conclusions

The present work demonstrated that the precipitation manner in the Cu/SiO₂ catalysts prepared by DP method has wide effects on the texture, structure and composition of the dried, calcined and reduced catalysts. The copper species on the dried, calcined and reduced Cu/SiO₂ catalysts prepared by Hom-DP and Het-DP methods as well as on the catalysts after work were assigned based on characterizations and literature works. Due to a homogeneous precipitation manner, the Hom-DP catalyst presented a much higher dispersion, a smaller copper particle size and thus a larger copper surface area than those of the Het-DP catalyst. Nonetheless, catalytic tests in the hydrogenolysis of glycerol showed that the latter catalyst inversely surpassed the former catalyst. The better performance of Het-DP catalyst as compared to Hom-DP catalyst is mainly due to a larger number of copper species in the former catalyst was prereduced to active Cu⁰ sites, which also showed remarkable higher stability during the reaction. Moreover, the selectivity to 1,2-PDO product is found to be affected by both the precipitation agent applied and the structure of the catalysts. It is preferable to produce Cu/SiO₂ catalyst for glycerol reaction by Het-DP method, however, the catalytic performance of this catalyst still needs further improvement.

Acknowledgments

The authors gratefully acknowledge the technical assistance provided by Ms. L. He and Ms. L. Gao, and the financial support

from the National Natural Science Foundation of China (Grant 20973187).

References

- [1] T. Werpy, G. Petersen, *Top Value Added Chemicals from Biomass*, vol. 1, Results of Screening for Potential Candidates from Sugars and Synthesis Gas, US DOE Report, 2004.
- [2] C.-H. Zhou, J.N. Beltramini, Y.-X. Fan, G.Q. Lu, *Chem. Soc. Rev.* 37 (2008) 527–549.
- [3] Y. Zheng, X. Chen, Y. Shen, *Chem. Rev.* 108 (2008) 5253–5277.
- [4] J. Chaminand, L. Djakovitch, P. Gallezot, P. Marion, C. Pinel, C. Rosier, *Green Chem.* 6 (2004) 359–361.
- [5] M.A. Dasari, P.-P. Kiatsimkul, W.R. Sutterlin, G.J. Suppes, *Appl. Catal. A* 281 (2005) 225–231.
- [6] A. Perosa, P. Tundo, *Ind. Eng. Chem. Res.* 44 (2005) 8535–8537.
- [7] T. Miyazawa, Y. Kusunoki, K. Kunimori, K. Tomishige, *J. Catal.* 240 (2006) 213–221.
- [8] E.P. Maris, R.J. Davis, *J. Catal.* 249 (2007) 328–337.
- [9] I. Furikado, T. Miyazawa, S. Koso, A. Shima, K. Kunimori, K. Tomishige, *Green Chem.* 9 (2007) 582–588.
- [10] A. Alhanash, E. Kozhevnikova, I. Kozhevnikov, *Catal. Lett.* 120 (2008) 307–311.
- [11] L. Huang, Y.L. Zhu, H.Y. Zheng, Y.W. Li, Z.Y. Zeng, *J. Chem. Technol. Biotechnol.* 83 (2008) 1670–1675.
- [12] M. Akiyama, S. Sato, R. Takahashi, K. Inui, M. Yokota, *Appl. Catal. A* 371 (2009) 60–66.
- [13] M. Balaraju, V. Rekha, P.S.S. Prasad, B.L.A.P. Devi, R.B.N. Prasad, N. Lingaiah, *Appl. Catal. A* 354 (2009) 82–87.
- [14] L. Guo, J. Zhou, J. Mao, X. Guo, S. Zhang, *Appl. Catal. A* 367 (2009) 93–98.
- [15] T. Jiang, Y. Zhou, S. Liang, H. Liu, B. Han, *Green Chem.* 11 (2009) 1000–1006.
- [16] Z. Yuan, P. Wu, J. Gao, X. Lu, Z. Hou, X. Zheng, *Catal. Lett.* 130 (2009) 261–265.
- [17] J. Zhao, W. Yu, C. Chen, H. Miao, H. Ma, J. Xu, *Catal. Lett.* 134 (2010) 184–189.
- [18] L. Ma, D.H. He, *Catal. Today* 149 (2010) 148–156.
- [19] I. Gandarias, P.L. Arias, J. Requies, M.B. Güemez, J.L.G. Fierro, *Appl. Catal. B* 97 (2010) 248–256.
- [20] A. Bienholz, F. Schwab, P. Claus, *Green Chem.* 12 (2010) 290–295.
- [21] S. Wang, Y. Zhang, H. Liu, *Chem Asian J.* 5 (2010) 1100–1111.
- [22] Z. Yuan, L. Wang, J. Wang, S. Xia, P. Chen, Z. Hou, X. Zheng, *Appl. Catal. B* 101 (2011) 431–440.
- [23] C. Montassier, D. Giraud, J. Barbier, Polyol conversion by liquid phase heterogeneous catalysis over metals, in: M. Guisnet, J. Barrault, C. Bouchoule, D. Dupres, C. Montassier, G. Pérot (Eds.), *Stud. Surf. Sci. Catal.*, Elsevier, Amsterdam, 1988, pp. 165–170.
- [24] Z. Huang, F. Cui, H. Kang, J. Chen, X. Zhang, C. Xia, *Chem. Mater.* 20 (2008) 5090–5099.
- [25] Z. Huang, F. Cui, H. Kang, J. Chen, C. Xia, *Appl. Catal. A* 366 (2009) 288–298.
- [26] C.J.G. Van Der Grift, P.A. Elberse, A. Mulder, J.W. Geus, *Appl. Catal.* 59 (1990) 275–289.
- [27] G.L. Bezemer, P.B. Radstake, V. Koot, A.J. van Dillen, J.W. Geus, K.P. de Jong, *J. Catal.* 237 (2006) 291–302.
- [28] L.-F. Chen, P.-J. Guo, M.-H. Qiao, S.-R. Yan, H.-X. Li, W. Shen, H.-L. Xu, K.-N. Fan, *J. Catal.* 257 (2008) 172–180.
- [29] X. Tang, B. Zhang, Y. Li, Y. Xu, Q. Xin, W. Shen, *Appl. Catal. A* 288 (2005) 116–125.
- [30] X. Zhang, H. Wang, B.-Q. Xu, *J. Phys. Chem. B* 109 (2005) 9678–9683.
- [31] C.J.G. Van Der Grift, A.F.H. Wielers, B.P.J. Jogh, J. Van Beunum, M. De Boer, M. Versluijs-Helder, J.W. Geus, *J. Catal.* 131 (1991) 178–189.
- [32] E.D. Guerreiro, O.F. Gorriiz, J.B. Rivarola, L.A. Arrúa, *Appl. Catal. A* 165 (1997) 259–271.
- [33] T. Toupance, M. Kermarec, J.-F. Lambert, C. Louis, *J. Phys. Chem. B* 106 (2002) 2277–2286.
- [34] G. Díaz, R. Pérez-Hernández, A. Gómez-Cortés, M. Benaissa, R. Mariscal, J.L.G. Fierro, *J. Catal.* 187 (1999) 1–14.
- [35] X.G. Wen, Y.T. Xie, C.L. Choi, K.C. Wan, X.Y. Li, S.H. Yang, *Langmuir* 21 (2005) 4729–4737.
- [36] T. Toupance, M. Kermarec, C. Louis, *J. Phys. Chem. B* 104 (2000) 965–972.
- [37] T.M. Yurieva, G.N. Kustova, T.P. Minyukova, E.K. Poels, A. Bliiek, M.P. Demeshkina, L.M. Plyasova, T.A. Krieger, V.I. Zaikovskii, *Mater. Res. Innovations* 5 (2001) 3–11.
- [38] K.V.R. Chary, K.K. Seela, G.V. Sagar, B. Sreedhar, *J. Phys. Chem. B* 108 (2004) 658–663.
- [39] A. Auroux, A. Gervasini, C. Guimon, *J. Phys. Chem. B* 103 (1999) 7195–7205.
- [40] X.-C. Zheng, S.-P. Wang, S.-R. Wang, S.-M. Zhang, W.-P. Huang, S.-H. Wu, *Mater. Sci. Eng. C* 25 (2005) 516–520.
- [41] G.G. Jernigan, G.A. Somorjai, *J. Catal.* 147 (1994) 567–577.
- [42] A.J. Marchi, J.L.G. Fierro, J. Santamaría, A. Monzón, *Appl. Catal. A* 142 (1996) 375–386.
- [43] E.D. Guerreiro, O.F. Gorriiz, G. Larsen, L.A. Arrúa, *Appl. Catal. A* 204 (2000) 33–48.
- [44] F.-W. Chang, W.-Y. Kuo, K.-C. Lee, *Appl. Catal. A* 246 (2003) 253–264.
- [45] M. Balaraju, V. Rekha, P.S.S. Prasad, R.B.N. Prasad, N. Lingaiah, *Catal. Lett.* 126 (2008) 119–124.